THE JOURNAL OF COMPARATIVE NEUROLOGY 348:403–418 (1994)

GABAergic Terminals in Nucleus Magnocellularis and Laminaris Originate From the Superior Olivary Nucleus

E.A. LACHICA, R. RÜBSAMEN, AND E.W RUBEL
Virginia Merril Bloedel Hearing Research Center, Department of Otolaryngology-Head and Neck Surgery, University of Washington, Seattle, Washington 98195

ABSTRACT

The auditory brainstem nuclei, angularis (NA), magnocellularis (NM), and laminaris (NL) of the chicken, *Gallus*, contain terminals that stain for antibodies against the inhibitory neurotransmitter, gamma-aminobutyric acid (GABA). Some of these terminals originate from cells surrounding nucleus magnocellularis. Results from this study indicate that the *majority* of the GABAergic terminals found in NA, NM and NL originate from the superior olivary nucleus (SON). Injections of cholera toxin and horseradish peroxidase show that superior olivary nucleus (SON) neurons, which respond to pure tones, project bilaterally to NA, NM and NL. NA and NL are reciprocally connected with the SON. More NA cells project to the SON than NL cells. While SON neurons project to NM, NM neurons do not project axons back to the SON. The configuration of SON terminals in NA, NM and NL matches the pattern of GABA-immunoreactive puncta seen in these three nuclei: they surround individual NM cells, congregate in the dendritic neuropil of NL, and blanket the NA. The data indicate that NA, NM and NL may be affected by two different inhibitory cell types: local interneurons and SON neurons. Patterns of connectivity described in this report suggest that the activity of NA cells could influence NM and NL cell physiology. Specifically, increases in NA cell activity could augment the effects of GABAergic SON neurons on NM and NL. Hence, binaural perception in the chicken may be more dependent upon changes in intensity cues than previously believed.

Key words: parallel pathways, cochlear nucleus, inhibition, auditory system, cholera toxin

In avians, axons from the auditory nerve bifurcate to form excitatory ipsilateral connections with the large round cells in nucleus magnocellularis (NM) and the stellate-shaped cells located in nucleus angularis (NA; Boord, 1969; Parks and Rubel, 1978; Jhaveri and Morest, 1982a,b). NM neurons project bilaterally to nucleus laminaris (NL), a sheet of cells whose dendritic branches are polarized dorsally and ventrally (Boord, 1969; Parks and Rubel, 1975; Smith and Rubel, 1979; Young and Rubel, 1983). Ipsilaterally projecting NM axons form excitatory connections with the dorsal dendrites of laminaris cells, while contralaterally projecting collateral branches form excitatory synapses with the ventrally directed dendrites (Rubel and Parks, 1975; Young and Rubel, 1983, 1986). NA neurons do not project to NL. Instead, their ascending axons form connections with a number of structures (Conlee and Parks, 1986; Takahashi and Konishi, 1988b), the most prominent of which is the dorsal lateral mesencephalic nucleus (MLd). Intercalated among the excitatory connections made between the auditory nerve and NM and NA neurons, and excitatory connections between NM axons and NL neurons, is a dense network of terminals containing the inhibitory neurotransmitter, gamma-aminobutyric acid, GABA (Code et al., 1989; Carr et al., 1989; von Bartheld et al., 1989). Where do these GABA-containing terminals originate from?

Results from a previous study from our laboratory revealed that stellate cells surrounding the chicken NM and NL stained positively for GABA (von Bartheld et al., 1989). A similar distribution of GABA-immunoreactive interneurons has also been described in the barn owl (Carr et al., 1989). It has been argued that these cells provide some of the GABAergic terminations ending on magnocellularis and laminaris neurons. This small population of GABA-staining neurons may not account completely for the dense network of terminals present in NM and NL. GABA-positive terminals are also present in NA, and the origin of these terminals is not known.

Accepted April 18, 1994.

Address reprint requests to E.W Rubel, Virginia Merril Hearing Research Center, Department of Otolaryngology-Head and Neck Surgery, University of Washington, Seattle, WA 98195.

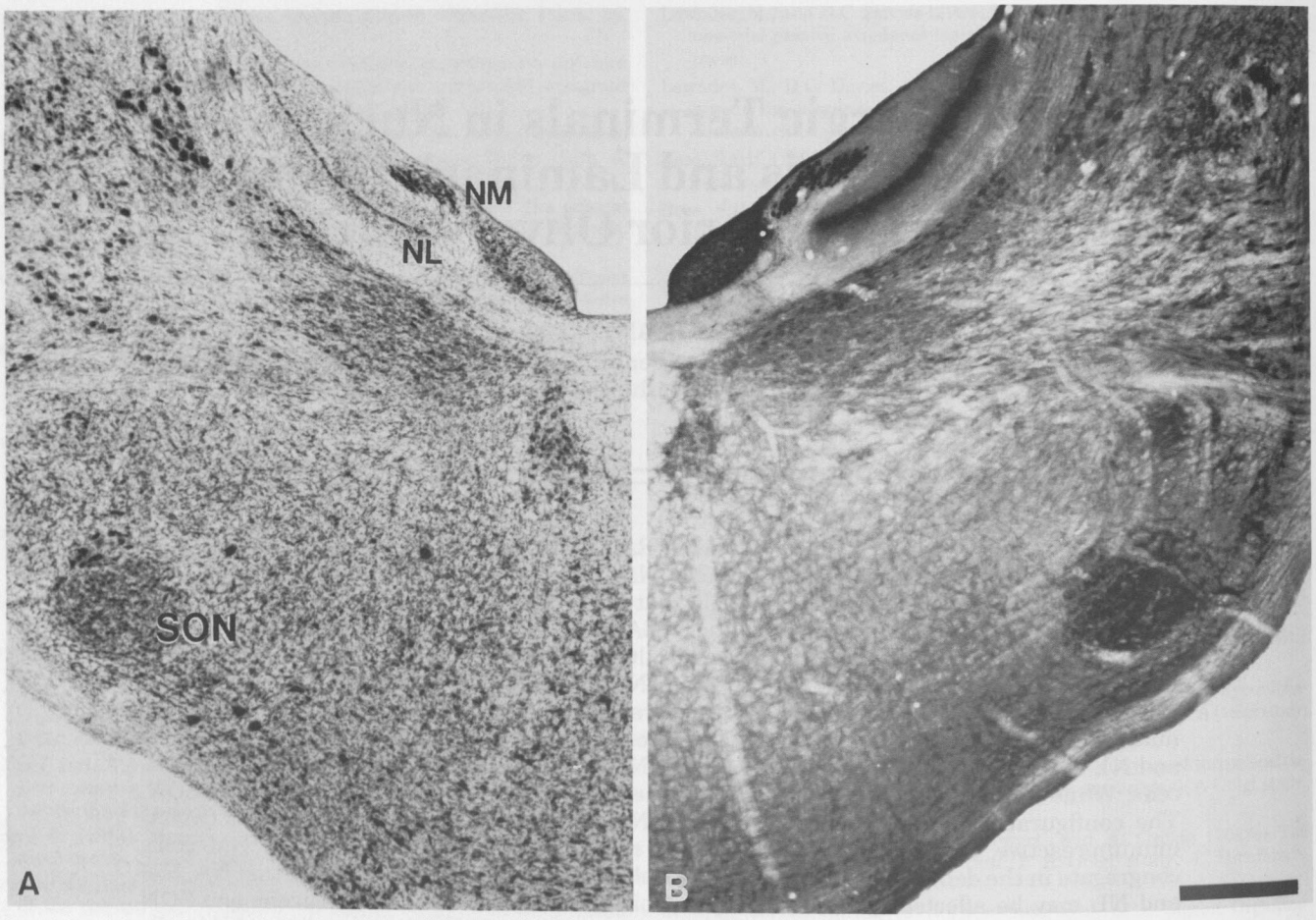

Fig. 1. Nucleus magnocellularis, nucleus laminaris, and the superior olivary nucleus (SON) are shown stained for Nissl (**A**) and cytochrome oxidase (**B**). The olive is easy to detect in cytochrome oxidase-stained sections as a dark round ball. The SON does not stain evenly for cytochrome oxidase: the ventral lateral half of the nucleus stains more intensely than the dorsal medial cap. NM, n. magnocellularis; NL, n. laminaris; SON, superior olivary nucleus. Scale bar = 500 μm.

A second reason for conducting this study revolved around the puzzling finding of a decrease in GABAergic terminal staining in nucleus magnocellularis contralateral to a cochlear removal (Code et al., 1990); the intensity of GABA-immunoreactive staining of terminals located in the ipsilateral, or deafferented NM was not altered. A reduction in the staining intensity of GABA terminals ending on NM neurons contralateral to its deafferented counterpart indicates that GABAergic cells in the opposite side of the medulla can detect changes in neural activity associated with deafferentation. Other investigators have argued that this alteration in GABA terminal staining is due to a reduction in the activity of the neurons that stimulate the GABAergic stellate cells (Code et al., 1990). This hypothesis was not tested, however, because the afferents to these GABAergic neurons have never been identified (von Bartheld et al., 1989).

There are alternative explanations for the reduction in GABA terminal staining. First, the GABA neurons surrounding the deafferented NM may not be interneurons. Instead, they may project to the opposite (i.e., the innervated) NM. If this were the case, then it could be assumed that the GABAergic stellate cells are afferent to auditory nerve collaterals. Secondly, another source of GABAergic neurons might exist that are located on the deafferented side of the brainstem, but project to the afferented side of the medulla. Either one of these possibilities can be directly tested by making a large injection of a retrogradely transported marker into nucleus magnocellularis.

Using anterograde and retrograde tracing techniques we present evidence indicating that a third-order auditory structure, the superior olivary nucleus (SON) is a major source of GABAergic terminals found in NA, NM and NL in the chicken. This conclusion is based on immunohistochemical data which reveals that the SON is composed of cells that are GABA-immunoreactive and connectional evidence showing that the pattern of SON axonal terminations in NA, NM and NL is similar to the pattern of GABAergic terminal staining seen in these nuclei.

MATERIALS AND METHODS

Recording and injection procedures

The data were acquired from 40 white leghorn hatchling chickens (*Gallus gallus*) between 9 and 12 days old. These birds were anesthetized with a mixture of Ketaset (0.75 mg/kg) and xylazine (0.5 mg/kg) diluted 1:1 in bacteriostatic saline. Supplemental anesthesia was administered at half the original dose every 60 minutes. Once the bird was anesthetized its skull was exposed by making a single

longitudinal incision and reflecting the skin and connective tissue laterally. A small metal post was then attached to the rostral pole of the skull with dental cement. This post was used to secure the animal's head to a custom made stereotaxic apparatus (see Rübsamen et al., 1988, 1989). With the bird's head firmly secured in the head-holder, a single small craniotomy (less than 500 μm diameter) was performed approximately 5 mm lateral to the midline of the skull above the cerebellum, followed immediately with a durotomy. Multiple penetrations were made through this hole with the electrode tilted 12° laterally by systematically moving the electrode in the rostrocaudal plane in steps of one or two degrees. Glass micropipettes filled with 3 M KCl (impedance of 1–4 MΩ) served as recording electrodes.

Auditory responses were evoked from nucleus magnocellularis and the superior olivary nucleus by ipsilateral stimulation with pure tones. Acoustic stimulation (100 ms in duration; 5 msec rise-fall time) was applied at intensities ranging from 10 to 105 dB SPL with frequencies between 100 to 5,000 Hz. Stimulus frequency and attenuation were varied manually during target search. Once the target nucleus was located response areas of multiunit clusters (and occasionally of single units) were acquired from spike discharges to pure tone stimuli presented in a pseudorandom sequence of different frequencies and intensities. Each frequency-intensity combination was presented three times in a predefined frequency-intensity array. Test sounds were generated with an IBM compatible laboratory computer (Compaq 386/20) equipped with a 12-bit D/A converter (Neuroboard, custom design). Absolute stimulus intensity was set by computer controlled attenuators. The same device was also used to correct for the band-specific frequency response of the speaker (for details see: Knipschild et al., 1992).

Multiple penetrations were made in order to physiologically determine the borders of the target structure. Once Cartesian coordinates defining the mediolateral, dorsoventral and rostrocaudal boundaries of the nucleus were assigned, the recording electrode was removed and replaced with an injection pipette filled with either 20% horseradish peroxidase (HRP), 1% HRP conjugated to cholera toxin (CTb-HRP), or 1% unconjugated choleragenoid (CTb). Both the conjugated and unconjugated forms of cholera toxin (List Biologicals) and HRP (Type VI, Sigma) were diluted in 10 mM phosphate-buffered saline (PBS). The injection pipette was used to verify by electrophysiological recording the best frequency representation at the target site to ensure that the injection pipette was appropriately positioned.

HRP and CTb-HRP were expelled iontophoretically from the glass pipette (40–50 μm I.D.) using 1 to 5 μA of constant current for a period of 20 to 30 minutes. The unconjugated choleragenoid was pressure-injected from a glass pipette (40–50 μm I.D.) for a similar duration (at 1 pulse/sec) using a Picospritzer (General Valve, E. Hanover, NJ). At the end of these procedures the animal was removed from the head-holder and placed in a warmed cage to recover from the effects of anesthesia, which took 60 minutes or less. Birds had free access to food and water.

Every measure was taken to ensure the comfort and safety of the chicken during and after the experiment. The treatment of all the animals used in this study was approved by the Committee for Animal Care at the University of Washington. In addition, animal care guidelines set forth by the Society for Neuroscience were strictly observed.

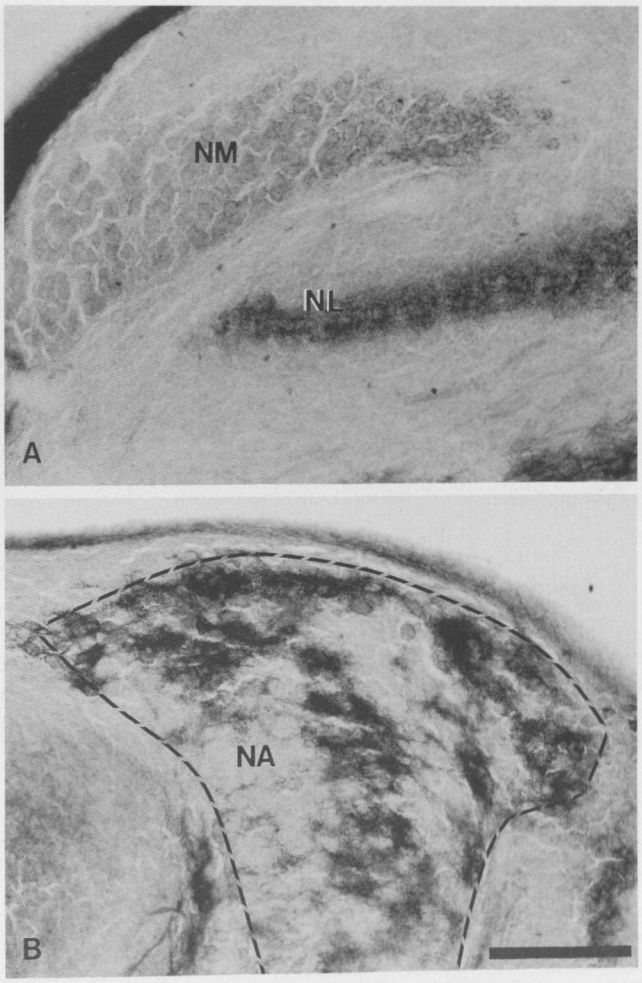

Fig. 2. Nucleus magnocellularis and n. laminaris (**A**) and nucleus angularis (**B**) are shown stained for antibodies against GABA. Few GABA immunoreactive cell bodies are seen in these nuclei; GABA immunoreactive terminals predominate. Labelled terminals surround individual magnocellularis cells and individual puncta can be discriminated. The density of stained terminals is greater in n. laminaris and n. angularis. NM, n. magnocellularis; NL, n. laminaris; NA, n. angularis. Scale bar = 250 μm.

Fixation, histological procedures

Subjects were given a lethal dose of pentobarbital 12 to 18 hours after the tracer injection, then fixed via transcardial perfusion of 2.5% glutaraldehyde and 1% formaldehyde buffered by 0.1 M sodium phosphate. Animals injected with CTb survived for 2.5 days before they were killed and then fixed with 4% formaldehyde in 0.1 M phosphate buffer. In every case, aldehyde fixatives were followed by a solution of 20% sucrose (in phosphate buffer). The brain was removed, then blocked at the level of the MLd rostrally and the nucleus of the glossopharyngeal nerve caudally. This block was frozen immediately and 60 μm thick sections were cut using a sliding microtome. HRP and CTb-HRP were visualized, respectively, by incubating freely floating sections in diaminobenzidine (DAB; Adams, 1981) or tetra methyl benzidine (TMB; Gibson et al., 1984). Unconjugated choleragenoid was visualized immunocytochemically using DAB as a chromogen following procedures supplied by List Biologicals; alternate sections in the CTb-processed series

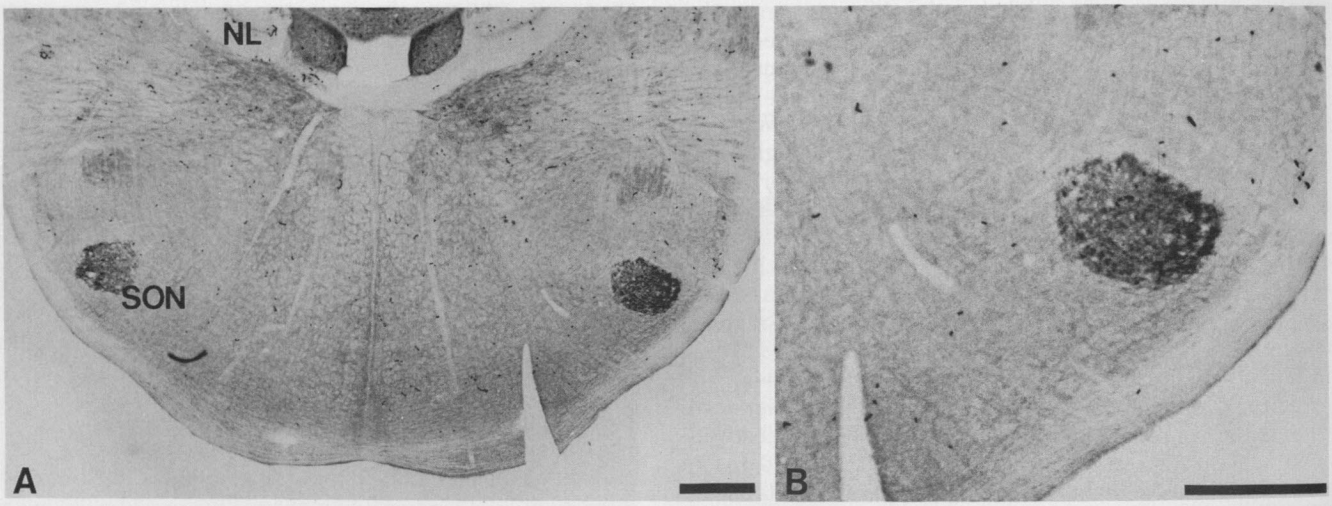

Fig. 3. **A:** Photomicrograph of a coronal section through the brainstem containing the superior olivary nucleus (SON) immunostained for glutamic acid decarboxylase (GAD). **B:** The same nucleus at a higher magnification. Scale bars = 500 μm.

were stained for Nissl substance. All sections were mounted on glass slides and dried at room temperature. Later, these sections were dehydrated through an ascending ethanol series, cleared in xylene and coverslipped using Permount.

Neurocytochemical procedures

A pair of 10-day-old hatchling chickens were overdosed with pentobarbital, then fixed via transcardial perfusion of 10% formalin in 5% sucrose-phosphate buffer. The brainstem was removed and blocked, then sectioned on a vibratome at 60 μm. Alternate sections were stained for Nissl substance and cytochrome oxidase (CO) following a modified version of Wong-Riley's method (1979). Sections stained for CO were first pretreated for 24 hours at less than 0°C in 30% ethylene glycol/30% sucrose in phosphate buffer. These sections were rinsed several times in 10 mM phosphate-buffered saline before incubating in the CO solution.

Four hatchling chickens, approximately 10 days old, were used to determine whether the SON contained GABA-immunoreactive cells. Each bird was given a lethal dose of pentobarbital then fixed via transcardial perfusion of a mixed aldehyde solution containing 2% glutaraldehyde and 0.1% formaldehyde. A block of the brainstem containing the medullary auditory nuclei was removed and cut into 40 μm thick sections with a vibratome. Alternate sections were mounted on glass slides, stained for Nissl substance, dehydrated, cleared and coverslipped as described above. The remaining sections were treated to block endogenous peroxidase activity then exposed to an antibody (diluted 1:4,000 in PBS and 3% normal goat serum) raised against GABA (INStar). The following morning the GABA antibody (Ab) was removed and replaced with a biotinylated linking Ab (goat anti-rabbit, diluted 1:250 in PBS). The antigen-antibody complexes were visualized subsequently with a VectaStain ABC kit (Vector Laboratories) using DAB as the chromogen.

Finally, three 10-day-old hatchling chickens were anesthetized and fixed as described above; each animal's brainstem was removed, sectioned on a vibratome, and immunostained for Abs against glutamic acid decarboxylase (GAD) raised from a hybridoma (ATCC, HB-184). GAD Abs were visualized using DAB as a chromogen following methods described by Gottlieb et al. (1986).

Soma size analyses

The area of GABA-immunoreactive and Nissl-stained neurons were measured at 63× in five nonoverlapping traverses through single sections taken at the caudal, rostral and intermediate levels of the SON using the BioQuant Morphometric Analysis system (R&M Biometrics). This resulted in measurements of 150 to 300 neurons in each brain. The soma area of SON cells labelled by HRP or CTb were also measured in the same fashion.

RESULTS

Located in the avian brainstem are four auditory nuclei: nucleus magnocellularis, nucleus angularis, nucleus laminaris, and the superior olivary nucleus. NM and NA are second-order auditory nuclei which receive excitatory input from auditory nerve fibers; NL and the SON are third-order auditory structures. NL receives excitatory input from NM neurons. The SON, which is composed of small cells (254 $\mu m^2 \pm 57$ μm^2; s.d.) that stain intensely for Nissl and CO (see Fig. 1), receives input from both NA and NL neurons (Conlee and Parks, 1986; Takahashi and Konishi, 1988b).

All four of these nuclei stain intensely for antibodies against GABA. NM, NA and NL contain few GABAergic cells; most of GABA immunolabel seen in these three nuclei exists in the form of terminal puncta. Photomicrographs of NM, NL and NA immunostained for GABA are shown in Figure 2. In NM, GABAergic terminals appear as small pock-like marks that surround individual neurons (Fig. 2A). NL is invested more heavily with GABA terminals which end on laminaris somata and coat the dorsal and ventral dendrites (Fig. 2A). NA appears to have the greatest investment of GABA terminations, blanketing NA neurons as well as the surrounding neuropil (Fig. 2B).

The SON, in addition to containing GABA- and GAD-immunopositive terminals, contains a large number of GABA-immunoreactive cells (Fig. 3). Nearly 70% of the cells in the SON stained positively for GABA. It is possible

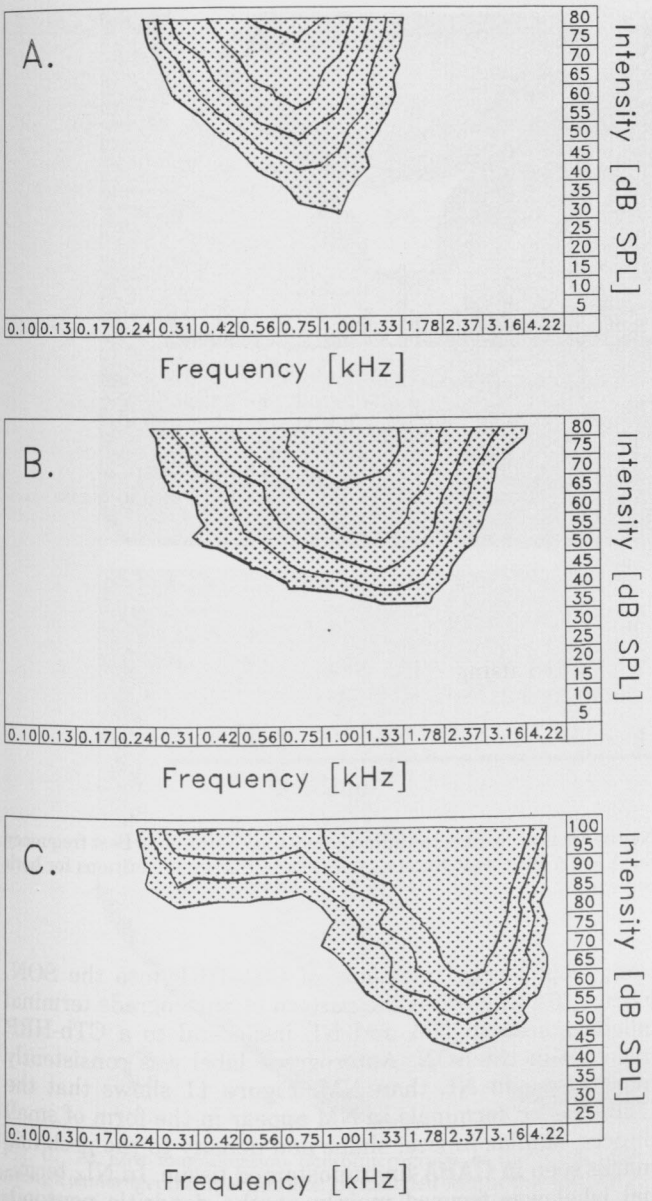

Fig. 4. **A–C:** Representative frequency/threshold curves for three different neurons in the superior olivary nucleus.

that some of the cells that did not stain for GABA were glial cells or glycinergic neurons (Schwarz et al., 1993). Hence, the SON, like the mammalian dorsal nucleus of the lateral lemniscus, for example, (Adams and Mugnaini, 1984; Shneiderman et al., 1988), may be comprised of, almost exclusively, GABAergic projection cells.

Physiological responses of SON neurons

While the major goal of this study was to examine the connections of the SON, in the course of studying its descending projections we were able to examine the physiological properties of 24 individual olivary neurons (from 8 birds). While a thorough description of SON physiology was beyond the scope of this study, several of their evoked and unevoked responses are worthy of mention.

SON neurons responded vigorously to pure tone stimulation with latencies ranging from 5 to 8 msec. Figure 4 shows frequency/threshold curves for 3 representative SON neurons. In general, SON neurons had well defined best frequencies (BFs) that ranged between 0.3 and 3 kHz. It is noteworthy that the frequency/threshold curves for neurons with BFs above 2 kHz showed distinct "low frequency tails" (Fig. 4C). Although the temporal properties of these cells were not studied in detail, it was apparent that neurons with BFs below 1 kHz did not phase-lock to the stimulus period as well as NM neurons with comparable BFs.

Figure 5 shows peristimulus time histograms for two different cells and illustrates three major features of SON neurons. First, many neurons discharged tonically to pure tone stimuli (see Fig. 5A). An equivalent number of neurons discharged vigorously at the onset of stimulus, firing less and less frequently, in a tonic/phasic manner, throughout the remainder of the stimulus presentation (see Fig. 5B). Finally, the majority of cells encountered showed a high rate of spontaneous activity (Fig. 5A). Other neurons were not spontaneously active (Fig. 5B).

Retrograde labelling of SON neurons

To determine whether SON cells projected to NM and NL, large deposits of HRP or CTb were placed into the tectal portion of the brainstem. These injection sites typically included the NM, NL and NA, and in some cases the medial and ventral vestibular nuclei (VeM and VeD, respectively [Karten and Hodos, 1967]).

Figure 6 shows a representative example of a very large deposit of CTb. The injection site included NM and NL (see Fig. 6A), as well as a portion of the VeM. CTb did not spread into NA or the VeD. Figure 6B shows NM and NL contralateral to the injection site. As expected, NM cells were well labelled, while NL cell bodies were not. Stellate cells located in the neuropil surrounding the contralateral NM and NL were never labelled. This observation indicates that GABAergic stellate cells are interneurons, effecting their actions unilaterally. Hereafter, these GABAergic cells will be referred to as interneurons. As shown in Figures 6C and D, large deposits of either HRP or CTb labelled cells in the ipsilateral and contralateral superior olivary nucleus.

Having demonstrated that SON cells possessed descending projections, small injections of HRP or CTb were made into NM and NL to determine whether descending SON axons ended on both NM and NL cells. A representative example of a HRP injection site restricted to NM is shown in Figure 7A. The degree to which the HRP was restricted to NM and did not spill into NL can be appraised by examining NM contralateral to the injection site: had HRP intruded into NL, arcuate NM fibers would have taken up the HRP and transported it back to its parent cell, specifically, an NM cell contralateral to the injection site. As Figure 7B shows, the magnocellular nucleus contralateral to the injection site did not contain any labelled somata (cf. Fig. 8B).

HRP was injected into NM in 6 birds. CTb was injected into the NM of 3 other birds. In each of these cases, retrogradely labelled cells were seen in the SON ipsilateral and contralateral to the injection site. Labelled SON cells possessed a multipolar morphology, emitting three to four primary dendrites (Fig. 7C and D). Although the tonotopy of the SON was not examined physiologically, it was clear from the results of HRP and CTb injections that the caudal portion of NM received input from the caudal portion of the

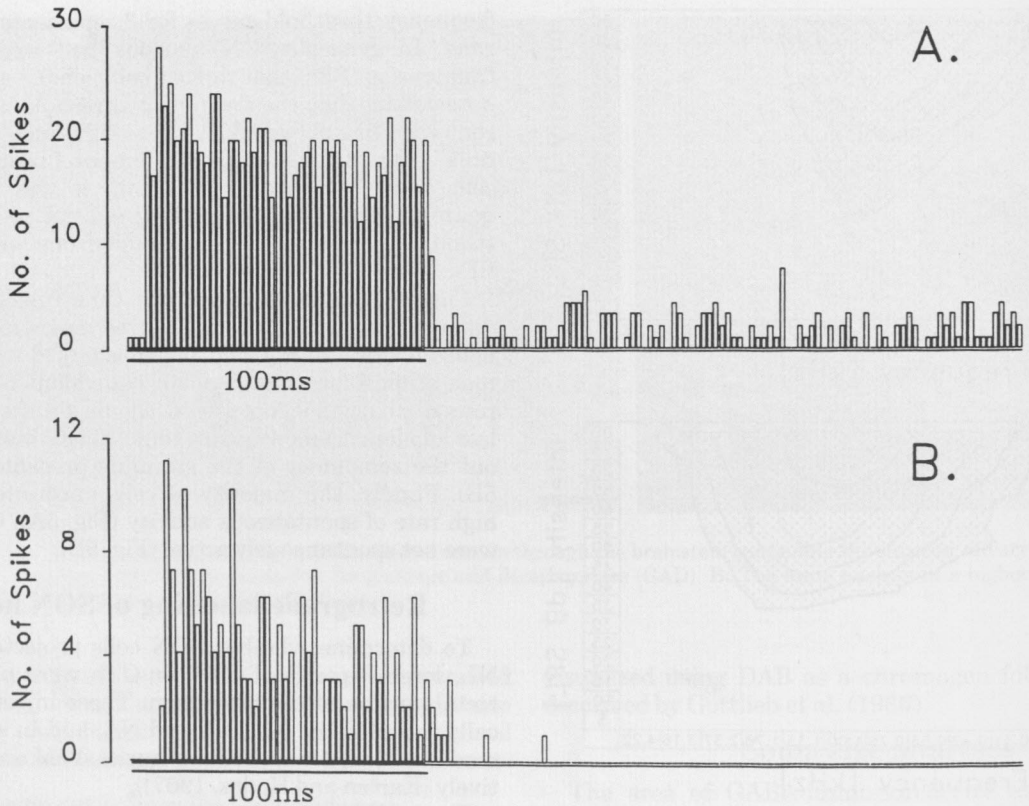

Fig. 5. **A, B:** Peristimulus time histograms for two different olivary neurons, one which continually discharged in the presence of the auditory stimulus, the other which responded in a phasic manner. Neither neuron responded immediately to the stimulus. Best frequency for A = 1.7 kHz; best frequency for B = 0.8 kHz. Repetitions for both cases = 20.

SON, while rostrally located SON cells projected to the rostral sites of NM.

Small deposits of HRP were made in NL in 4 birds; 2 other birds were injected with CTb. A representative example of a NL injection site is shown in Figure 8A. Figure 8B shows NM and NL on the opposite side of the medulla. As expected, injections into NL filled contralateral NM cells, as well as the arcuate NM axons that arborize on the ventral dendrites of NL cells. Like injections of HRP into NM, tracer injections into NL filled cells in the SON bilaterally. Additionally, ascending axons that ended in the SON were labelled. Figure 8C shows an example of HRP-filled ascending NL axons projecting to the SON; these axons arborized, roughly, in the medial half of the SON. In cases where CTb was used as a marker, however, CTb-immunopositive cells and terminals were distributed evenly throughout the SON. Anterogradely labelled CTb-positive terminals were also distributed evenly in the contralateral SON. As Figure 8C illustrates, laminaris cell axons ending in the SON were collateral branches of arcuate fibers that coursed through the lamino-olivary tract en route to the dorsal-lateral mesencephalic nucleus. In every case, axonal arbors in the SON could be traced back to a collateral from an axon in the lamino-olivary tract.

Anterograde labelling of SON terminals

Unilateral injections of CTb-HRP were made into the SON of 3 birds to determine whether SON axonal terminals ending in NM and NL were configured in a manner that resembled the pattern of GABAergic terminal staining (see Fig. 1). Figure 9A and B show, at low and higher magnification, respectively, injections of CTb-HRP into the SON. Figure 10A illustrates the pattern of anterograde terminal labelling seen in NM and NL ipsilateral to a CTb-HRP injection in the SON. Anterograde label was consistently more dense in NL than NM. Figure 11 shows that the CTb-labelled terminals in NM appear in the form of small puncta, similar in size, shape and density to the pock-like marks seen in GABA-immunostained tissue. In NL, terminal label was focused mainly on the dendritic neuropil. Terminal labelling was not seen on NL cells bodies (Fig. 11B). Figure 10B shows the NM and NL contralateral to a CTb-HRP injection in the SON: a similar pattern and density of anterogradely labelled terminals is seen in the contralateral nuclei; the only possible difference was that the density of anterogradely labelled terminals seemed greater in the contralateral NM and NL than the ipsilateral nuclei. Counts of SON neurons labelled by large injections of HRP and CTb into NM and NL do not support this observation, however. On average, more labelled neurons were found in the ipsilateral SON (1.7× more) compared to the contralateral SON. Figure 10B also shows that labelled terminals were present in contralateral NA; the ipsilateral NA contained a similar density of labelled terminals. Finally, injections of CTb-HRP also labelled terminals in the contralateral SON (not illustrated).

Anterogradely transported markers have been used by others to show that both NA and NL project to the SON (Conlee and Parks, 1986; Takahashi and Konishi, 1988b). Our results replicate and extend these findings by showing that unilateral injections of CTb into the SON produced retrogradely labelled cells in the ipsilateral and contralat-

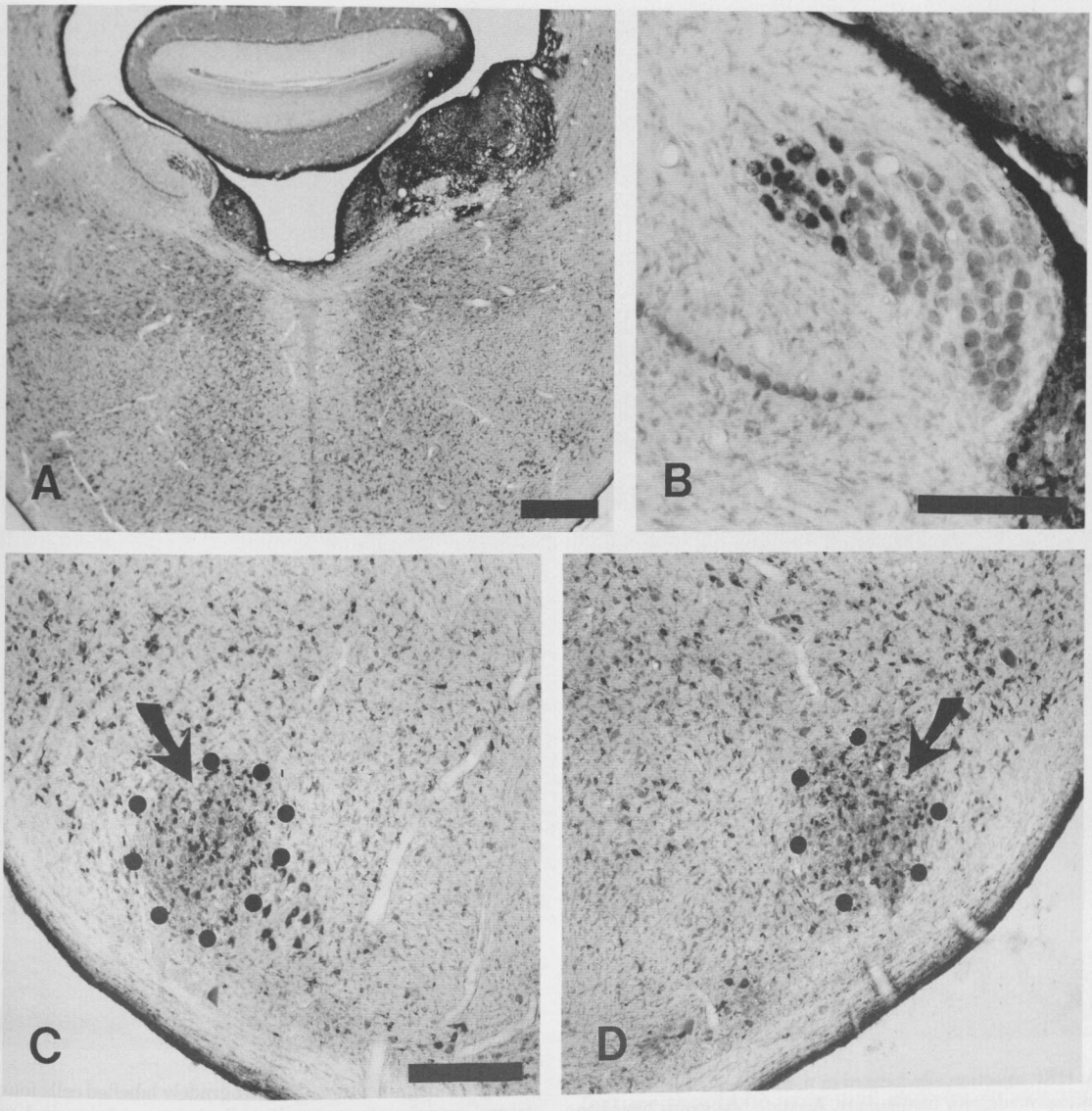

Fig. 6. **A:** Low magnification photomicrograph of the brainstem showing a choleragenoid injection site. **B:** Labelled cells in the contralateral nucleus magnocellularis (NM). Only magnocellularis neurons were labelled; stellate cells that surround NM (which are immunoreactive for GABA) were not labelled. **C, D:** Labelled cells in the superior olivary nuclei (arrows) ipsilateral and contralateral to the injection site, respectively. The section was counterstained for Nissl substance. Scale bars = 1 mm in A, 250 μm in B, 500 μm in C, D.

eral NA and NL. These CTb injections also showed that the ipsilateral nuclei contained more labelled cells than contralateral nuclei. Finally, more NA neurons projected to the SON than NL neurons (see Fig. 12).

Soma size comparisons

The histograms shown in Figure 13 compare the mean soma size of Nissl-stained SON neurons, GABA-immunoreactive neurons, and neurons retrogradely filled with HRP or CTb following injections of these tracers into both NM and NL (error bars are S.D.). We chose to pool NM- and NL-backfilled SON cells in our analyses because a priori comparisons of NM-filled vs. NL-filled SON neurons revealed that the two groups did not differ statistically in soma size (data not shown). As seen in Figure 13, the soma size distributions of retrogradely labelled SON cells were comparable to the distributions obtained from GABA-immunoreactive or Nissl-stained cells, in spite of differences in tissue processing.

DISCUSSION

Nucleus magnocellularis, n. laminaris and n. angularis contain terminals that are immunoreactive for antibodies against GABA and GAD (Code et al., 1989; von Bartheld et al., 1989; Carr et al., 1989). We present evidence indicating that the majority of these GABAergic terminals originate from neurons in the superior olivary nucleus; previous studies have shown that the SON projects bilaterally to the MLd (Conlee and Parks, 1986; Takahashi and Konishi, 1988a). This is the first report to describe in detail the descending projections of the SON. Our main results can be summarized as follows: (1) the SON is composed of cells that stain intensely for Nissl, cytochrome oxidase, and antibodies raised against GABA; (2) olivary neurons respond to stimuli after a long latency, indicating that they do not receive direct input from the auditory nerve; (3) the SON is not physiologically homogeneous: some cells are spontaneously active, others are not; some cells respond

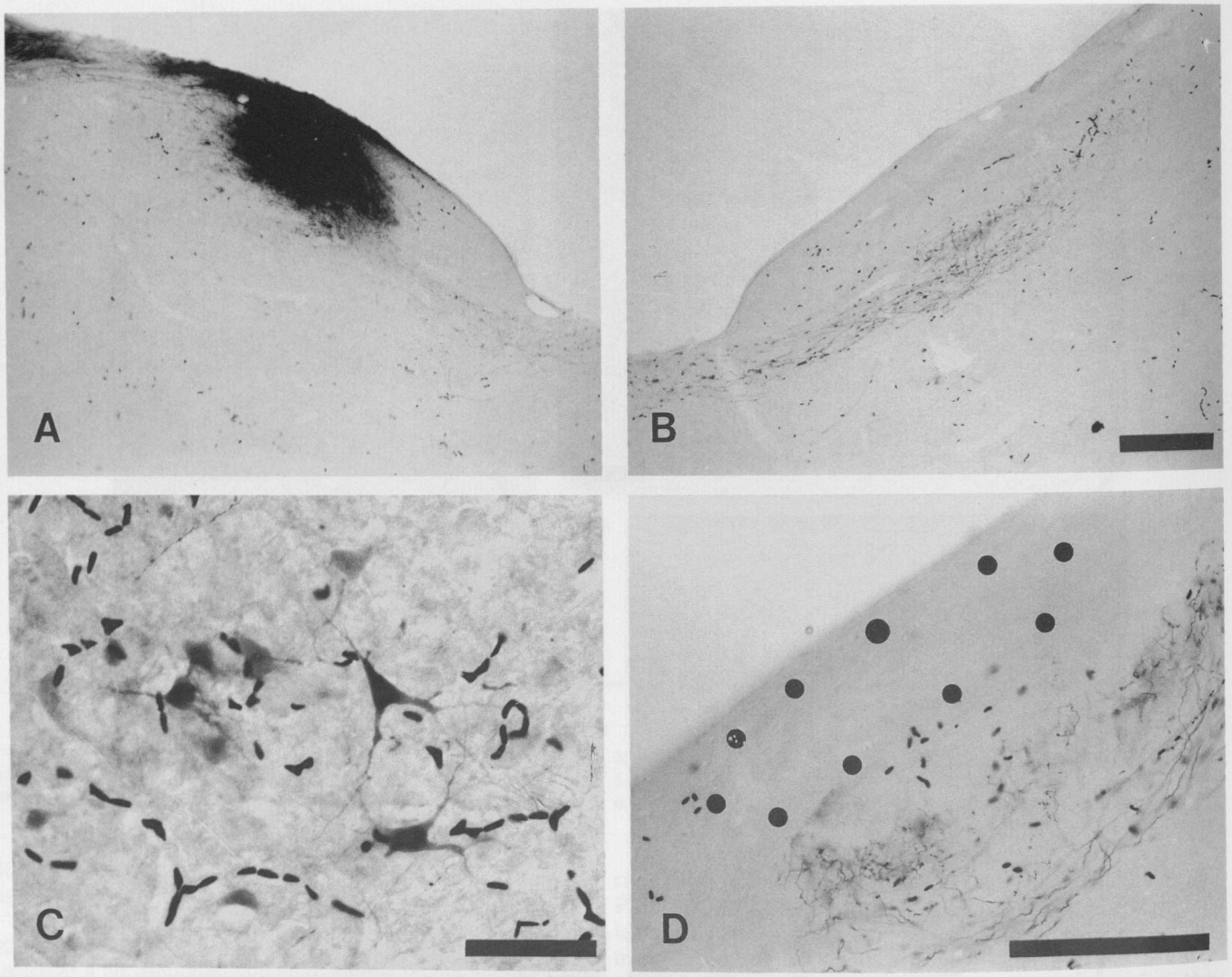

Fig. 7. **A:** HRP injection site located in n. magnocellularis (NM). **B:** The contralateral medullary hemisphere. Arcuate NM axons have been anterogradely labelled, but there are no retrogradely labelled neurons in the contralateral NM. **D:** The contralateral nucleus (marked by dots) at higher magnification. **C:** Retrogradely labelled cells found in the ipsilateral superior olivary nucleus. Scale bars = 1 mm in A and B, 250 μm in C, 20 μm in D.

tonically to pure tones, others in a tonic/phasic manner; (4) the SON receives bilateral input from n. angularis and n. laminaris cells with the homolateral nuclei providing more input than the contralateral nuclei; (5) more NA cells project to the SON than NL cells; and (6) cells in the SON project bilaterally to NA, NM and NL. A caricature of the chicken brainstem is illustrated in Figure 14 showing the connections of the SON that have been revealed in this report, along with the ascending projections linking the papilla with the central auditory nuclei that have been described previously (Conlee and Parks, 1986; Takahashi and Konishi, 1988a).

The evidence to support the claim that GABAergic terminals in NA, NM and NL originate from the SON is indirect. At the present time, double-labelling studies have not been conducted because available fluorescent probes are vulnerable to glutaraldehyde fixation required to perform GABA immunohistochemistry. Nevertheless, the idea that GABA-containing terminals originate from SON neurons is fortified by the following results. The SON contains an abundance of GABAergic cells. Over 70% of the neurons are estimated to be immunoreactive for GABA. This fact, coupled with the observation that large injections of retrograde tracers into NM, NA and NL label SON neurons, indicates that GABAergic SON cells must project to these structures. A similar connection between the SON and NM has been described in the barn owl (Carr et al., 1989). The finding that best supports our claim is the observation that SON terminals end in a pattern that matches the distribution of GABAergic endings seen in NM, NL *and* NA.

We argued previously that all GABAergic terminals originated from neurons found in the neuropil surrounding NM and NL (von Bartheld et al., 1989). The size of the interneuron population, estimated to be between 100 and 200 neurons, is rather small. All of the GABAergic endings found in NM and NL could be attributed to a small number of neurons if they possessed widely spreading dendritic or axonal branches (or both), heavily laden with boutons. This

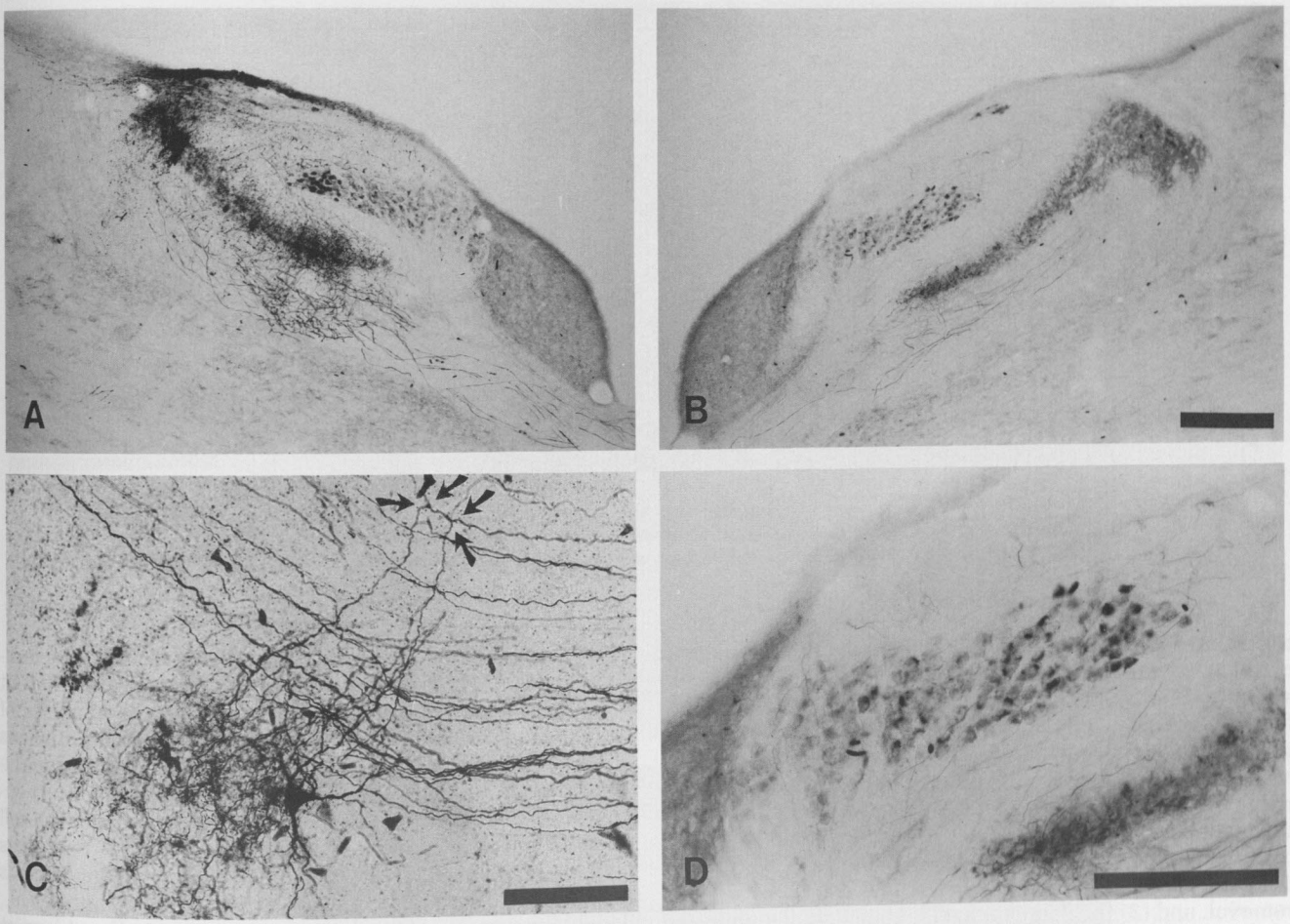

Fig. 8. **A:** HRP injection sites in n. laminaris (NL). **B:** Contralateral medullary hemisphere where both arcuate axons and n. magnocellularis neurons have been labelled. **D:** Labelled neurons at higher magnification. **C:** HRP-filled NL axons ending in the superior olivary nucleus (SON; arrows show collateral points); an HRP-labelled SON cell is also seen in C. Scale bars = 1 mm in A and B, 250 μm in C, 25 μm in D.

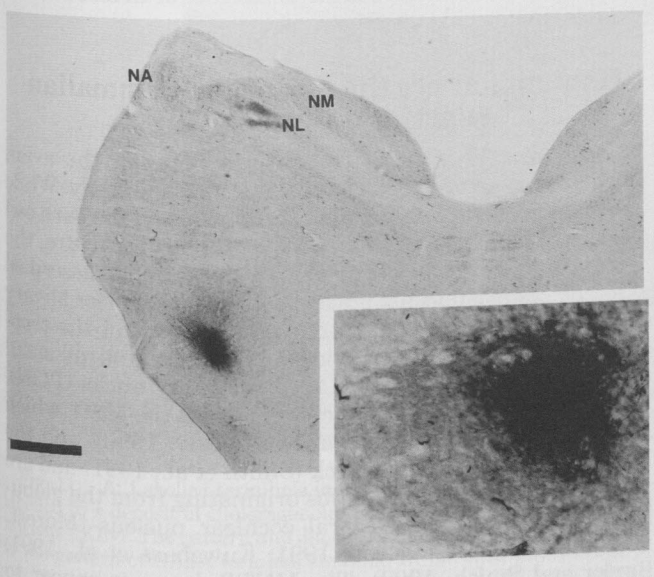

Fig. 9. This section, containing nucleus magnocellularis, n. angularis, and n. laminaris, shows a CTb-HRP injection located in the superior olivary nucleus. The core of the injection site is shown in the **inset** (magnified 140×). NA, n. angularis; NM, n. magnocellularis; NL, n. laminaris. Scale bar = 1 mm.

feature should be examined in order to acquire a complete understanding of GABAergic influences on these brainstem auditory nuclei.

Additional support for the view that the SON is the chief source of inhibitory input to NM, NL and NA, is provided by the fact that SON cells can be activated directly by angularis or laminaris neurons. The afferents to GABA interneurons have yet to be identified. The dendritic "shortcomings" of n. magnocellularis (Jhaveri and Morest, 1982a,b) and n. laminaris neurons (Smith and Rubel, 1979) prevent them from activating the majority of interneurons which are found in satellite positions around NM and NA. It is possible that some interneurons could be stimulated by collaterals of auditory nerve axons. This seems unlikely because the collateral branches of auditory nerve axons do not arborize in the neuropil that surrounds the cochlear nuclei (Parks and Rubel, 1978; Carr and Boudreau, 1991; Jhaveri and Morest, 1982a). Other possibilities are stimulation by NM or NA axon collaterals (which have not been described), or stimulation by axons originating from SON neurons (which have not been examined).

The bilateral projections of the SON may help us understand the curious effect that a cochlear removal has on GABA terminal immunoreactivity in NM. Briefly, a reduction in the number of GABA-staining terminals in the

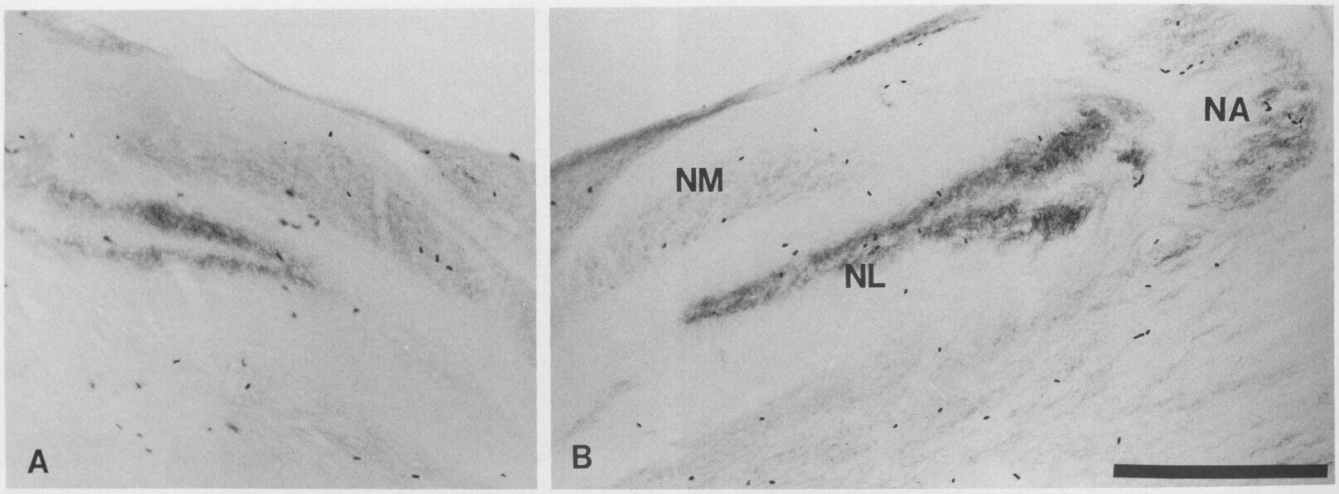

Fig. 10. Following injections of CTb-HRP into the superior olivary nucleus, anterogradely labelled terminals are seen in n. magnocellularis and n. laminaris both ipsilateral (**A**) and contralateral (**B**) to the injection site. Labelled terminals are also seen in n. angularis. NA, n. angularis; NM, n. magnocellularis; NL, n. laminaris. Scale bar = 1 mm.

contralateral NM is seen several days after unilateral cochlear removal (Code et al., 1990). This result may be accounted for by the deafferentation of *n. angularis* which forms a robust projection with the SON, which, in turn projects to the contralateral NM (see Fig. 14). In this regard, it should be noted that unilateral cochlear removal results in a marked reduction in 2-deoxyglucose (2-DG) in the ipsilateral SON (Lippe et al., 1980). These three results [that is: (1) the bilateral projections of the SON to NM, (2) the reduction of 2-DG in the SON ipsilateral to cochlear removal, and (3) the decrease in GABA terminal staining in NM contralateral to a unilateral cochlear removal] suggest that the SON may project more heavily to the contralateral rather than the ipsilateral NM. This issue needs to be examined more closely.

Previous studies (von Bartheld et al., 1989; Carr et al., 1989) and the data communicated here indicate that neurons in NM, NL and NA are subject to two sources of inhibition: from SON neurons as well as local interneurons. This is not an unusual scenario. In fact, this design appears to be a ubiquitous feature of sensory system nuclei. In mammals, for example, projection neurons of thalamic sensory nuclei are contacted by GABAergic interneurons (Penny et al., 1983, 1984; Thompson et al., 1985; Wenthold et al., 1986; Harris and Hendrickson, 1987; Williams and Faull, 1987; Winer and Larue, 1988) as well as GABAergic cells in the thalamic reticular nucleus (Montero and Scott, 1981; Rouiller et al., 1985; Ohara et al., 1989; Conley and Diamond, 1990; Houser et al., 1980; Conley et al., 1991; Oertel et al., 1983). Sensory cortical areas, in addition to possessing a complement of inhibitory interneurons, are affected by GABAergic cells in the zona incerta (Lin et al., 1990). GABA- and glycinergic projection nuclei appear to be the rule, rather than the exception in the auditory system: consider, for example, the dorsal nucleus of the lateral lemniscus and its projections to the inferior colliculus (Adams and Mugnaini, 1984; Shneiderman et al., 1988; Shneiderman and Oliver, 1989), or the medial nucleus of the trapezoid body whose cells project chiefly to the lateral superior olivary nucleus (LSO) (Glendenning et al., 1985, 1991; Spangler et al., 1985; Sanes et al., 1987; Zook and DiCaprio, 1988; Sanes, 1990; Kuwabara et al., 1991).

The two sources of inhibition could be viewed as redundant. Alternatively, the two sources may have very different effects on their targets. Electron microscopic analyses of cells located in the mammalian lateral geniculate nucleus (LGN) indicate that the actions of the two GABA populations may differ: GABA terminals originating from interneurons end on dendritic segments that are proximal to the cell body or on presynaptic endings, while GABA terminals originating from neurons of the thalamic reticular nucleus end on distal portions of the same dendrite (Ohara et al., 1980; Lindstrom, 1983; Hamos et al., 1985; Cucchiaro et al., 1991). The overall pattern of GABA-labelled terminals, and the pattern of efferent SON terminations in NL suggests that such a disparity exists in NL as well: SON terminals do not appear to end on NL cell bodies, which appear to be postsynaptic to an abundance of GABA-stained endings (Code et al., 1989).

How similar are the avian and mammalian superior olivary nuclei?

Unfortunately a direct comparison between the avian and mammalian olivary nuclei cannot be made easily. While the superior olivary nucleus of the chicken and the barn owl appears to be a cytoarchitectonically distinct structure, the mammalian structure of the same name is better described as a complex of 3 distinct nuclei [the medial superior olivary nucleus (MSO), the LSO, the medial nucleus of the trapezoid body (MNTB)] embedded in a reticulum of small nuclei, collectively known as the periolivary nuclei (PON). The SON shares the least in common with the MSO, which is homologous to nucleus laminaris (Carr, 1990), and the MNTB, whose cells phase-lock (Smith et al., 1991) and are postsynaptic to large end bulbs originating from the globular cells of the anteroventral cochlear nucleus (Morest, 1968; Kuwabara and Zook, 1991; Kuwabara et al., 1991; Banks and Smith, 1992). The MNTB does not appear to have an avian homologue. The SON shares a few features in common with the LSO, including bilateral projections to the mesencephalon (Glendenning et al., 1981, 1985; Glendenning and Masterton, 1983) and cells that are immunoreactive for antibodies raised against inhibitory transmitters

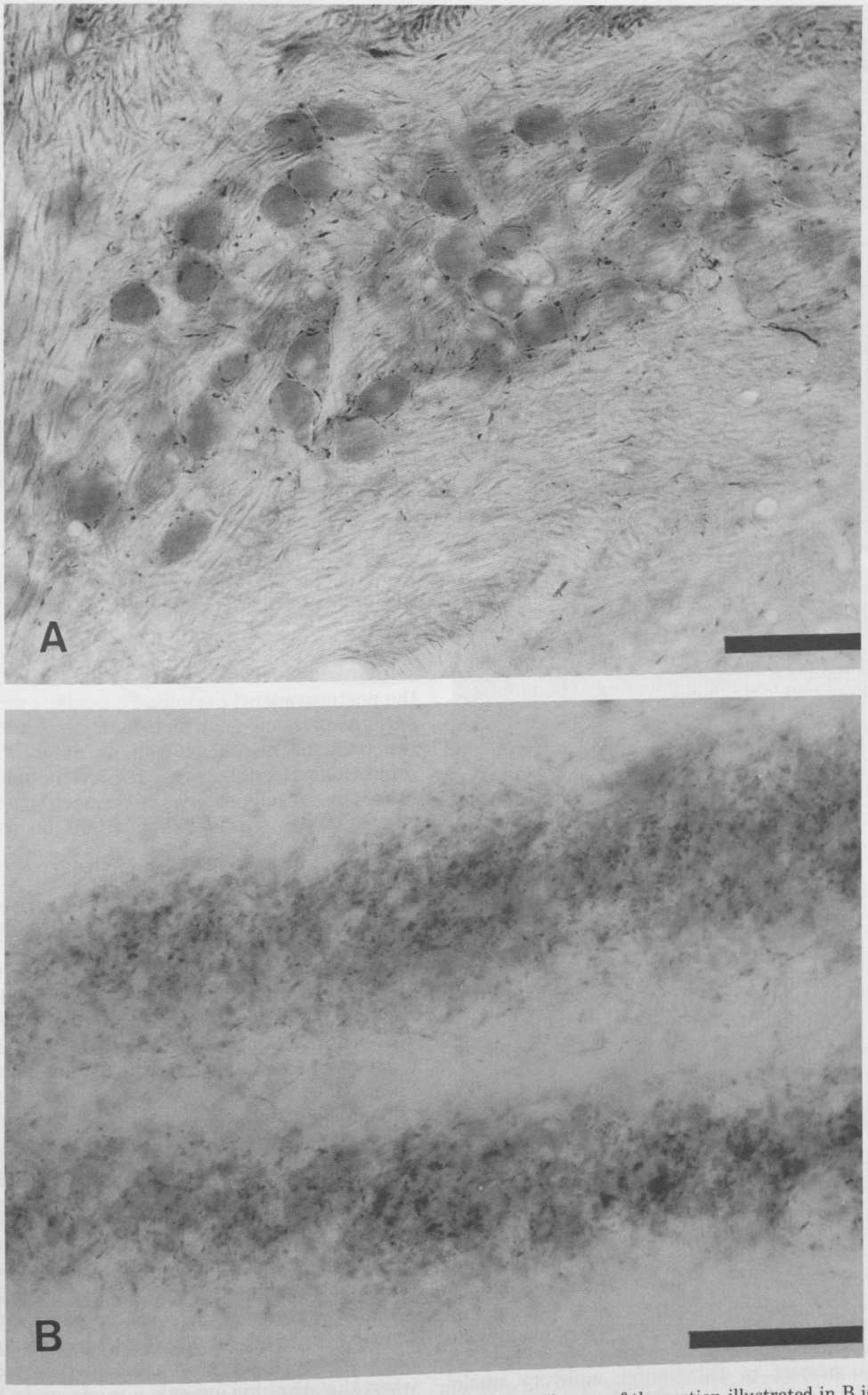

Fig. 11. **A:** Labelled terminals in n. magnocellularis, anterogradely labelled by a deposit of choleragenoid in the ipsilateral superior olivary nucleus (SON). The pattern and density of labelled terminals is similar to the pattern of GABA terminal staining. **B:** Labelled terminals in n. laminaris. The cut of the section illustrated in B is oblique; thus, the nucleus appears to be more than a monolayer thick. The oblique cut, however, provides an aspect which reveals that SON terminals congregate in the dendritic neuropil only. Scale bars = 100 μm.

(Roberts and Ribak, 1987; Helfert et al., 1989). Although they may not be regarded as strictly homologous, we propose that the avian SON is most similar to the mammalian PON.

PON cells, like SON cells, stain positively for inhibitory neurotransmitters such as GABA and glycine (Thompson et al., 1985; Schwartz and Yu, 1986; Helfert et al., 1989; Benson and Potashner, 1990), possess diffuse descending

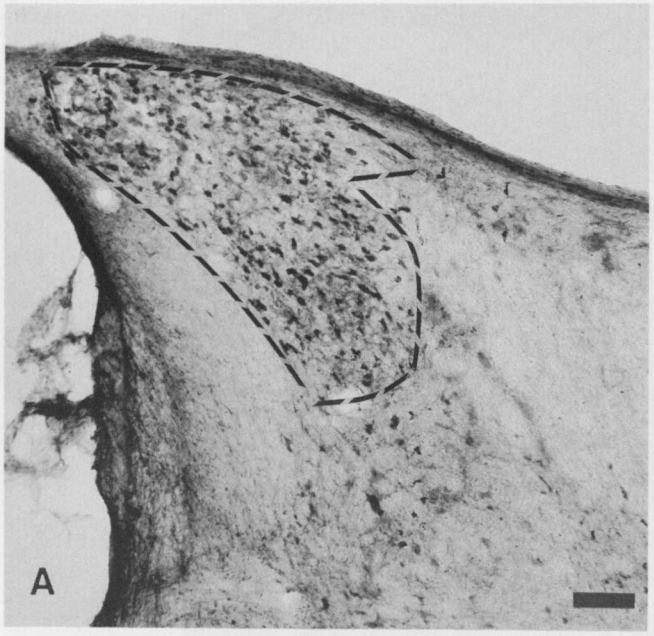

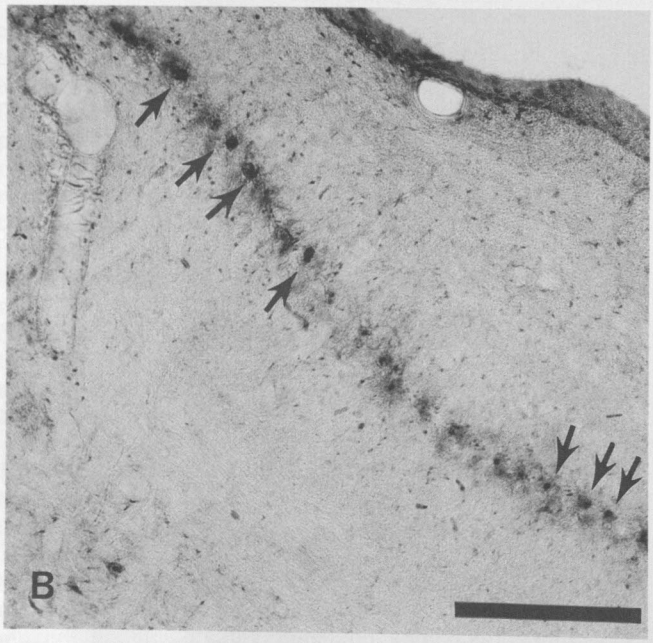

Fig. 12. Many labelled cells are seen in n. angularis (NA) following deposits of retrogradely transported markers into the superior olivary nucleus (SON). **A:** Labelled cells in NA (borders marked by dashed lines) contralateral to the SON injected with HRP. **B:** Retrogradely labelled cells in the ipsilateral n. laminaris (small arrows). Scale bars = 250 μm.

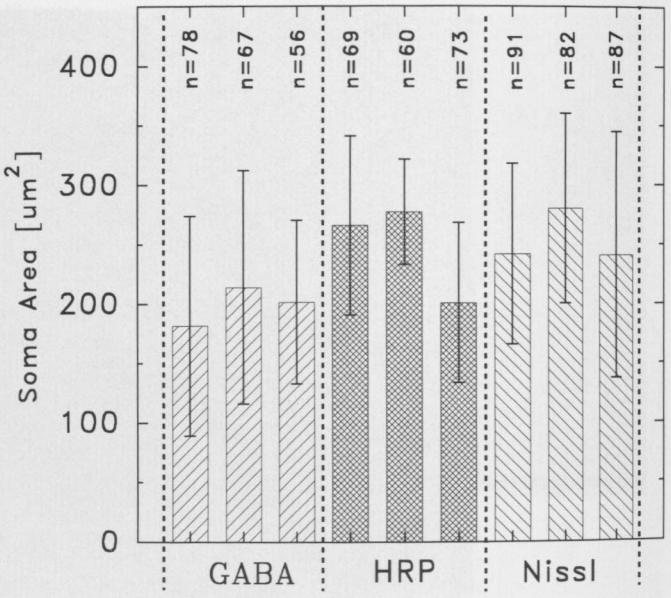

Fig. 13. These histograms illustrate that the somatic areas of neurons in the superior olivary nucleus stained for Nissl, GABA, and HRP or choleragenoid are all very similar.

projections to cochlear nuclei (Spangler et al., 1987; Schofield, 1991), project to third-order auditory nuclei (Spangler and Warr, 1991; Cant, 1991; Banks and Smith, 1992; Cant and Hyson, 1992), and project to the inferior colliculus (Warr, 1966; Helfert et al., 1988; Schofield, 1991; Schofield and Cant, 1992). No one single periolivary subnucleus, in particular, should be considered homologous to the avian SON, because no single nucleus duplicates perfectly the pattern of projections demonstrated by the SON. Some nuclei, such as the superior periolivary nucleus, the ventral and lateral nucleus of the trapezoid body are more similar in their connectivity to the SON than, for example, the posteroventral periolivary nucleus or the anterolateral periolivary nucleus, which lack descending projections to the cochlear nuclei as well as ascending mesencephalic projections (Spangler et al., 1987; Schofield and Cant, 1992). Since the overall patterns of connectivity between the SON and PON are similar, they might be considered as field homologues.

What role might the SON play in central auditory processing?

In order to consider possible roles for the SON, specific physiological features of the nuclei that the SON projects to need to be recapitulated. Unfortunately, single unit response properties of NL neurons have not been well-characterized in the chicken. Hence, the discussion that follows focuses mainly on the possible effects that the SON may have on NM and NA neurons which differ markedly in their responses to auditory stimuli (Rubel and Parks, 1975; Sachs and Sinnott, 1978; Sullivan and Konishi, 1984; Warchol and Dallos, 1990).

NA cells are morphologically and physiologically heterogeneous. Most NA neurons do not exhibit high rates of spontaneous activity, show relatively poor phase-locking, and have complex response areas with sideband inhibition. These cells often have relatively steep rate/intensity functions covering 30–50 dB. These growth functions are often nonmonotonic, showing a marked decrease in firing rate when the stimulus exceeds a moderately high level. Inhibitory afferents to NA provided by SON cells could contribute to the inhibitory sidebands and internal complexities of the NA cell response areas. In addition, SON projections may contribute to the inhibition of firing often observed at high stimulus intensity, since this particular feature cannot be readily attributed to auditory nerve axons. It is important to note that the NA is hodologically complex. As a result, the physiological properties of NA cells could be shaped by a variety of other descending inputs, as well as interneurons.

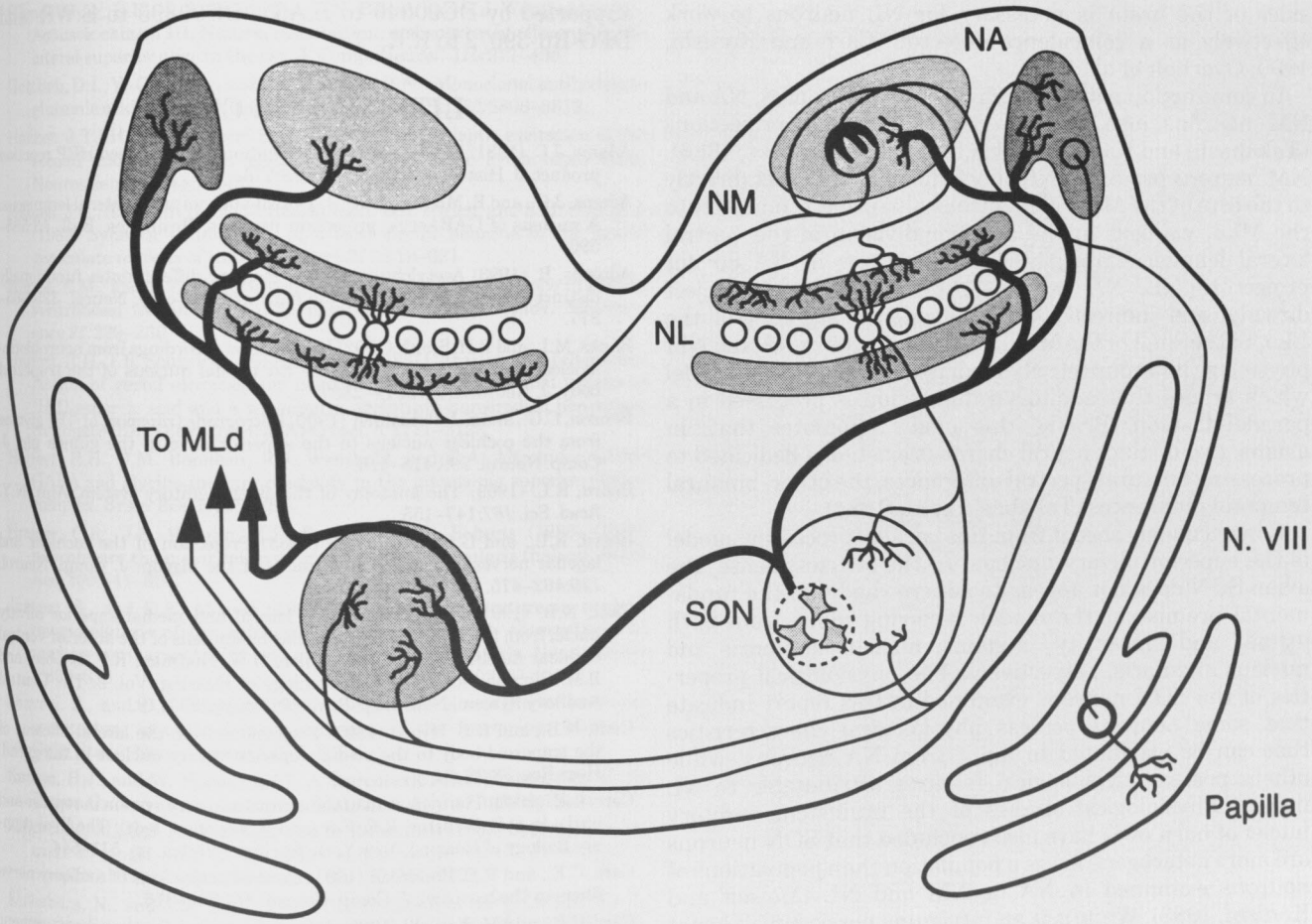

Fig. 14. The connections that link the cochlea to nucleus angularis (NA), n. magnocellularis (NM), n. laminaris (NL) and the superior olive (SON) are shown here. Connections that have been described previously, specifically, the unilateral projection of the auditory nerve to NA and NM, the bilateral projection of NM to NL and the bilateral ascending projections of NA and NL to the SON are depicted as thin lines. The bilateral ascending projections of NA and NL to the dorsal lateral mesencephalic nucleus (MLd) are not shown. Connections depicted by the thicker lines represent projections of the SON described in this report. The SON forms chiefly descending projections at this level of the auditory pathway, projecting back to NA, NM and NL bilaterally, and to the SON on the opposite side of the brainstem. The SON also projects forward to the MLd. The configuration of individual SON axon arbors is not known; as a result, SON termination patterns in individual nuclei are represented by gray shading. The number of nuclei that an individual SON neuron projects to is also not known; hence, the overall projection patterns of a network of GABAergic SON neurons (enclosed within the circle) are illustrated.

In contrast to NA, the neurons of NM are remarkably homogeneous in both morphology and physiology. Virtually all investigators agree that NM neurons display high rates of spontaneous activity and have primary-like response areas. In addition, NM neurons are exquisitely phase-locked, particularly in the barn owl. Curiously, responses of NM neurons to changes in stimulus intensity appear to markedly differ in different reports. In the barn owl, Sullivan and Konishi (1984) report that NM neurons have relatively flat rate/intensity functions and a limited dynamic range. In redwing blackbirds (Sachs and Sinnott, 1978) and chickens (Warchol and Dallos, 1990), however, the rate/intensity functions and the dynamic range of NM neurons were found to be comparable to those of NA neurons and eighth nerve axons. The reasons underlying this discrepancy are not known. One possibility is that a fundamental difference exists in the innervation of NM neurons between these species. This seems unlikely, however. In all cases the major (or only) excitatory afferents to NM neurons are 2–3 auditory nerve axons that end with large end bulbs of Held (Boord and Rassmusen, 1963; Parks and Rubel, 1978; Hacket et al., 1982; Jhaveri and Morest, 1982a; Parks, 1981; Carr and Boudreau, 1991).

A second explanation for these disparaties in intensity/rate functions might be related to differences in the anesthetic protocol used in each of the studies cited above. The barn owl recordings were conducted while animals were lightly anesthetized with a dissociative, ketamine (4 mg/kg/hr), while chicks and redwing blackbirds were treated with barbiturates or hypnotics, respectively. A plausible hypothesis is that the latter anesthetic agents affected the GABAergic interconnections between the SON and NM. In the absence of GABAergic influence, input/output functions of NM cells would be nearly identical to those of the auditory nerve axons. If this is the case, then the relatively shallow input/output functions described for NM neurons of the barn owl may be due to the GABAergic feedback described here. As it turns out, the SON is uniquely situated to analyze intensity information arriving at the two ears (via input from NA) and to modulate the binaural balance of activity in NM and NL. It seems likely that maintaining relatively equivalent inputs to NL cells from NM on the two

sides of the brain is necessary for NL neurons to work effectively as a coincidence detector (Carr and Konishi, 1990; Overholt et al., 1992).

In conjunction with their physiologic differences, NA and NM neurons also differ in their ascending projections (Takahashi and Konishi, 1988a,b; Conlee and Parks, 1986). NM neurons project to NL only, whose cells project directly to the core of the MLd. NL neurons also project indirectly to the MLd, via cells in the anterior division of the ventral lateral lemniscal nucleus (LLv). Neurons in NA do not project to NL. NA neurons, like NL neurons, project directly, and indirectly via the posterior segment of the LLv, to the shell of the MLd. The differences in NA and NM physiology and connectivity form the foundation of a model which argues that auditory information is processed in a parallel fashion. Briefly, this model stipulates that, in avians, two distinct neural channels exist: one dedicated to processing binaural spectral differences, the other, binaural temporal differences (Takahashi et al., 1984).

Conspicuously absent from this parallel processing model is the superior olivary nucleus. In the strictest sense, the avian SON does not appear to adhere rigidly to the fundamental premise of the model, receiving input from both "time" and "intensity" systems, nucleus laminaris and nucleus angularis, respectively. The physiological properties of the SON neurons examined in this report indicate that some neurons possess physiological characteristics that can be attributed to input from NA neurons, while others possess physiological features attributable to NL inputs. Physiological studies of the brainstem auditory nuclei of barn owls have also concluded that SON neurons are more heterogeneous as a population than populations of neurons examined in NA or NM and NL (Moiseff and Konishi, 1983). While it is an intriguing possibility, it is not possible, based on information, to determine if time and intensity information converge on single cells or are segregated in the SON. It could be argued that the SON is similar in its connectivity to the LLv, possessing subdivisions that receive, in a nonoverlapping fashion, inputs from NA and NL. There is circumstancial evidence to support this idea in the barn owl; specifically, it has been shown that the lateral portion of the barn owl SON stains very differently for cholinesterase than the media region (Adolphs, 1993). A similar difference is seen in the chicken SON stained for cytochrome oxidase. However, it is not known whether these neurochemically distinct sectors of the SON contain physiologically distinct neuronal types and different connectivity. Ultimately, a thorough understanding of the SON's role in central auditory processing, will depend on additional anatomical and physiological work. It would be of interest to know, for example, whether NA and NL inputs to the SON overlap, and whether SON neurons receiving input from NA or NL project specifically to their source of excitation.

ACKNOWLEDGMENTS

Drs. Bill Lippe, Harvey Karten and Alex Reyes contributed significantly to these experiments and the generation of this manuscript in the form of helpful discussion. Thanks to Drs. Catherine Carr and Rebecca Code for their thoughtful comments. We are especially indebted to Mr. Casey Cox at the University of California, San Diego, who performed outstanding immunohistochemical work on a pair of brains injected with choleragenoid. This work was supported by DC00040 to E.A.L., DC00395 to E.WR. and DFG-Ru-390/2 to R.R.

LITERATURE CITED

Adams, J.C. (1981) Heavy metal intensification of DAB-based HRP reaction product. J. Histochem. Cytochem. *29:*775.

Adams, J.C., and E. Mugnaini (1984) Dorsal nucleus of the lateral lemniscus: A nucleus of GABAergic projection neurons. Brain Res. Bull. *13:*585–590.

Adolphs, R. (1993) Acetylcholinesterase staining differentiates functionally distinct auditory pathways in the barn owl. J. Comp. Neurol. *329:*365–377.

Banks, M.I., and P.H. Smith (1992) Intracellular recordings from neurobiotin-labeled cells in brain slices of the rat medial nucleus of the trapezoid body. J. Neurosci. *12:*2819–2837.

Benson, C.G., and S.J. Potashner (1990) Retrograde transport of ^{3}[H] glycine from the cochlear nucleus to the superior olive in the guinea pig. J. Comp. Neurol. *296:*415–426.

Boord, R.L. (1969) The anatomy of the avian auditory system. Ann. N.Y. Acad. Sci. *167:*147–155.

Boord, R.L., and G.L. Rasmussen (1963) Projection of the cochlear and lagenar nerves on the cochlear nuclei of the pigeon. J. Comp. Neurol. *120:*462–475.

Cant, N.B. (1991) Projections to the lateral and medial superior olivary nuclei from the spherical and globular bushy cells of the anterior ventral cochlear nucleus. In R.A. Altschuler, D.W. Hoffman, R.P. Bobbin, and B.M. Clopton (eds): The Neurobiology of Hearing, Vol. 2, The Central Auditory System. New York: Raven Press, pp. 99–119.

Cant, N.B., and R.L. Hyson (1992) Projections from the lateral nucleus of the trapezoid body to the medial superior olivary nucleus in the gerbil. Hear Res. *58:*26–34.

Carr, C.E. (1990) The evolution of the central auditory system in reptiles and birds. In D.B. Webster, R.R. Fay, and A.N. Popper (eds): The Evolutionary Biology of Hearing. New York: Springer-Verlag, pp. 511–544.

Carr, C.E., and R.E. Boudreau (1991) Central projections of auditory nerve fibers in the barn owl. J. Comp. Neurol. *314:*306–318.

Carr, C.E., and M. Konishi (1990) Axonal delay lines for time measurement in the owl's brainstem. Proc. Natl. Acad. Sci. USA *85:*8311–8315.

Carr, C.E., I. Fujita, and M. Konishi (1989) Distribution of GABAergic neurons and terminals in the auditory system of the barn owl. J. Comp. Neurol. *286:*190–207.

Code, R.A., G.D. Burd, and E.W Rubel (1989) Development of GABA immunoreactivity in brainstem auditory nuclei of the chick: Ontogeny of gradients in terminal staining. J. Comp. Neurol. *284:*504–518.

Code, R.A., D. Durham, and E.W Rubel (1990) Effects of cochlea removal on GABAergic terminals in nucleus magnocellularis of the chicken. J. Comp. Neurol. *301:*643–654.

Conlee, J.W., and T.N. Parks (1986) Origin of ascending projections to the nucleus mesencephalicus lateralis pars dorsalis in the chicken. Brain Res. *367:*96–113.

Conley, M., and I.T. Diamond (1990) Organization of the visual sector of the thalamic reticular nucleus in Galago. Evidence that the dorsal lateral geniculate and pulvinar nuclei occupy separate tiers. Eur. J. Neurosci. *2:*211–226.

Conley, M., A.C. Kupersmith, and I.T. Diamond (1991) Organization of the auditory sector of the thalamic reticular nucleus in *Galago:* Comparison of the reciprocal connexions between the reticular nucleus and the ventral and magnocellular divisions of the medial geniculate complex. Eur. J. Neurosci. *3:*1089–1103.

Cucchiaro, J.B., D.J. Uhlrich, and S.M. Sherman (1991) Electron-microscopic analysis of synaptic input from the perigeniculate nucleus to the A-laminae of the lateral geniculate nucleus in cats. J. Comp. Neurol. *310:*316–336.

Gibson, A.R., D.I. Hansma, J.C. Houk, and F.R. Robinson (1984) A sensitive low artifact TMB procedure for demonstration of WGA-HRP in the CNS. Brain Res. *298:*235–241.

Glendenning, K.K., and R.B. Masterton (1983) Acoustic chiasm: Efferent projections of the lateral superior olive. J. Neurosci. *3:*1521–1537.

Glendenning, K.K., J.K. Brunso-Bechtold, G.C. Thompson, and R.B. Masterton (1981) Ascending auditory afferents to the nuclei of the lateral lemniscus. J. Comp. Neurol. *197:*673–703.

Glendenning, K.K., K.A. Huston, R.J. Nudo, and R.B. Masterton (1985) Acoustic chiasm II: Anatomical basis of binaurality in the lateral superior olive of cat. J. Comp. Neurol. *232:*261–285.

Glendenning, K.K., R.B. Masterton, B.N. Baker, and R.J. Wenthold (1991) Acoustic chiasm III: Nature, distribution, and sources of afferents to the lateral superior olive in the cat. J. Comp. Neurol. *310:*377–400.

Gottlieb, D.I., Y.-C. Chang, and J.E. Schwob (1986) Monoclonal antibodies to glutamic acid decarboxylase. Proc. Natl. Acad. Sci. *83:*8808–8812.

Hacket, J.T., H. Jackson, and E.W Rubel (1982) Synaptic excitation of the second and third order auditory neurons in the avian brain stem. Neuroscience *7:*1455–1469.

Hamos, J.E., S.C. Van Horn, D. Raczkowski, D.J. Ulrich, and S.M. Sherman (1985) Synaptic connectivity of a local circuit neurone in the lateral geniculate nucleus of the cat. Nature *317:*618–621.

Harris, R.M., and A.E. Hendrickson (1987) Local circuit neurons in the rat ventrobasal thalamus-a GABA immunocytochemical study. Neuroscience *21:*229–236.

Helfert, R.H., I.R. Schwartz, and A.F. Ryan (1988) Ultrastructural characterization of gerbil olivocochlear neurons based on differential uptake of ^{3}H-D-aspartic acid and a wheatgerm agglutinin-horseradish peroxidase conjugate from the cochlea. J. Neurosci. *8:*3111–3123.

Helfert, R.H., J.M. Bonneau, R.J. Wenthold, and R.A. Altschuler (1989) GABA and glycine immunoreactivity in the guinea pig superior olivary complex. Brain Res. *6:*269–286.

Houser, C.R., J.E. Vaughn, R.P. Barber, and E. Roberts (1980) GABA neurons are the major cell type of the nucleus reticularis thalami. Brain Res. *200:*341–354.

Jhaveri, S., and D.K. Morest (1982a) Neuronal architecture in nucleus magnocelluaris of the chicken auditory system with observations on nucleus laminaris: A light and electron microscope study. Neuroscience *7:*809–836.

Jhaveri, S., and D.K. Morest (1982b) Sequential alterations of neuronal architecture in nucleus magnocellularis of the developing chicken: A Golgi Study. Neuroscience *7:*837–853.

Karten, H.J., and W. Hodos (1967) A Stereotaxic Atlas of the Brain of the Pigeon *Colomba livia.* Baltimore, Maryland: Johns Hopkins Press.

Knipschild, M., G.J. Dorrscheidt, and R. Rübsamen (1992) Setting complex tasks to single units in the avian auditory forebrain I: Processing of complex artificial stimuli. Hearing Res. *57:*216–230.

Kuwabara, N., and J.M. Zook (1991) Classification of the principal cells of the medial nucleus of the trapezoid body. J. Comp. Neurol. *314:*707–720.

Kuwabara, N., R.A. DiCaprio, and J.M. Zook (1991) Afferents to the medial nucleus of the trapezoid body and their collateral projections. J. Comp. Neurol. *314:*684–706.

Linn, C.S., M.A. Nicolelis, J.S. Schneider, and J.K. Chapin (1990) A major direct GABAergic pathway from zona incerta to neocortex. Science *248:*1553–1556.

Lindstrom, S. (1983) Synaptic organization of inhibitory pathways to principal cells in the lateral geniculate nucleus of the cat. Brain Res. *234:*447–453.

Lippe, W.R., O. Steward, and E.W Rubel (1980) The effect of unilateral basilar papilla removal upon nuclei laminaris and magnocellularis of the chick examined with [^{3}H]2-deoxyglucose autoradiography. Brain Res. *196:*43–58.

Moiseff, A., and M. Konishi (1983) Characteristics of units in the owl's brainstem auditory pathway: precursors of restricted spatial receptive fields. J. Neurosci. *3:*2553–2562.

Montero, V.M., and G.L. Scott (1981) Synaptic terminals in the dorsal lateral geniculate nucleus from neurons of the thalamic reticular nucleus: A light and electron microscope autoradiographic study. Neuroscience *6:*2561–2577.

Morest, D.K. (1968) The growth of synaptic endings in the mammalian brain: A study of the calyces of the trapezoid body. Z. Anat. EntwGesch. *127:*201–220.

Oertel, W.H., A.M. Graybiel, E. Mugnaini, R.P. Elde, D.E. Schmechel, and I.J. Kopin (1983) Coexistence of gluatmic acid decarboxylase- and somatostatin-like immunoreactivity in neurons of the feline nucleus reticularis thalami. J. Neurosci. *3:*1322–1332.

Ohara, P.T., G. Chazal, and H.J. Ralston, III (1989) Ultrastructural analysis of GABA-immunoreactive elements in the monkey thalamic ventrobasal complex. J. Comp. Neurol. *283:*541–558.

Ohara, P.T., A.J. Sefton, and A.R. Lieberman (1980) Mode of termination of afferents from the thalamic reticular nucleus in the dorsal lateral geniculate nucleus of the rat. Brain Res. *197:*503–506.

Overholt, E.M., E.W Rubel, and R.L. Hyson (1992) A circuit for coding interaural time differences in the chick brainstem. J. Neurosci. *12:*1698–1708.

Parks, T.N. (1981) Morphology of axosomatic endings in the avian cochlear nucleus: Nucleus magnocellularis of the chicken. J. Comp. Neurol. *203:*425–440.

Parks, T.N., and E.W Rubel (1975) Organization and development of the brain stem auditory nuclei of the chicken: Organization of projections from nucleus magnocellularis to nucleus laminaris. J. Comp. Neurol. *164:*435–448.

Parks, T.N., and E.W Rubel (1978) Organization and development of the brain stem auditory nuclei of the chicken: Primary afferent projections. J. Comp. Neurol. *180:*439–448.

Penny, G.R., D. Fitzpatrick, D.E. Schmechel, and I.T. Diamond (1983) Glutamic acid decarboxylase-immunoreactive neurons and horseradish peroxidase-labeled projection neurons in the ventral posterior nucleus of the cat and *Galago senegalensis.* J. Neurosci. *3:*1868–1887.

Penny, G.R., M. Conley, D.E. Schmechel, and I.T. Diamond (1984) The distribution of glutamic acid decarboxylase immunoreactivity in the diencephalon of the opossum and rabbit. J. Comp. Neurol. *228:*38–56.

Roberts, R.C., and C.E. Ribak (1987) GABAergic neurons and axon terminals in the brainstem auditory nuclei of the gerbil. J. Comp. Neurol. *258:*267–280.

Rouiller, E.M., E. Colomb, M. Capt, and F. deRibaupierre (1985) Projections of the reticular complex of the thalamus onto physiologically characterized regions of the medial geniculate body. Neurosci. Lett. *53:*227–232.

Rubel, E.W., and T.N. Parks (1975) Organization and development of brain stem auditory nuclei of the chicken: Tonotopic organization of n. magnocellularis and n. laminaris. J. Comp. Neurol. *164:*411–434.

Rübsamen, R., G. Neuweiler, and K. Sripathi (1988) Comparative collicular tonotopy in two bat species adapted to movement detection, *Hipposideros speoris* and *Megaderma lyra.* J. Comp. Physiol. (A) *163:*271–285.

Rübsamen, R., G. Neuweiler, and G. Marimuthu (1989) Ontogenesis of tonotopy in inferior colliculus of a hipposiderid bat reveals postnatal shift in frequency code. J. Comp. Physiol. (A) *165:*755–769.

Sachs, M.B., and Sinnot, J.M. (1978) Responses to tones of single cells in the nucleus magnocellularis and nucleus angularis of redwinged blackbird. J. Comp. Physiol. *126:*347–361.

Sanes, D.H. (1990) An *in vitro* analysis of sound localization mechanisms in the gerbil lateral superior olive. J. Neurosci. *10:*3494–3506.

Sanes, D.H., W.A. Gerary, G.F. Wooten, and E.W Rubel (1987) Quantitative distribution of the glycine receptor in the auditory brainstem of the gerbil. J. Neurosci. *7:*3793–3802.

Schofield, B.R. (1991) Superior paraolivary nucleus in the pigmented guinea pig: Separate classes of neurons project to the inferior colliculus and the cochlear nucleus. J. Comp. Neurol. *312:*68–76.

Schofield, B.R., and N.B. Cant (1992) Organization of the superior olivary complex in the guinea pig: II. Patterns of projection from the periolivary nuclei to the inferior colliculus. J. Comp. Neurol. *317:*438–455.

Schwartz, I.R., and S.-M. Yu (1986) An anti-GABA antibody labels subpopulations of axonal terminals and neurons in the gerbil cochlear nucleus and superior olivary complex. Soc. Neurosci. Abstr. *12:*780.

Schwarz, D.W.F., I.E. Schwarz, and B. Westerberg (1993) Glycine-ergic neurons in the auditory brainstem of the chicken. Soc. Neurosci. Abstr. *19:*1203.

Shneiderman, A., and D.L. Oliver (1989) EM autoradiographic study of the projections from the dorsal nucleus of the lateral lemniscus: A possible source of inhibitory inputs to the inferior colliculus. J. Comp. Neurol. *286:*28–47.

Shneiderman, A., D.L. Oliver, and C.K. Henkel (1988) Connections of the dorsal nucleus of the lateral lemniscus: An inhibitory parallel pathway in the ascending auditory system? J. Comp. Neurol. *276:*188–208.

Smith, D.J., and E.W Rubel (1979) Organization and development of brain stem auditory nuclei of the chicken: Dendritic gradients in nucleus laminaris. J. Comp. Neurol. *186:*213–240.

Smith, P.H., P.X. Joris, L.H. Carney, and T.C.T. Yin (1991) Projections of physiologically characterized globular bushy cell axons from the cochlear nucleus of the cat. J. Comp. Neurol. *304:*387–407.

Spangler, K.M., and W.B. Warr (1991) The descending auditory system. In R.A. Altschuler, D.W. Hoffman, R.P. Bobbin, and B.M. Clopton (eds): The Neurobiology of Hearing, Vol. 2, The Central Auditory System. New York: Raven Press.

Spangler, K.M., W.B. Warr, and C.K. Henkel (1985) The projection of principal cells of the medial nucleus of the trapezoid body in the cat. J. Comp. Neurol. *238:*249–262.

Spangler, K.M., N.B. Cant, C.K. Henkel, G.R. Farley, and W. Bruce Warr (1987) Descending projections from the superior olivary complex to the cochlear nucleus of the cat. J. Comp. Neurol. *259:*452–465.

Sullivan, W.E., and M. Konishi (1984) Segregation of stimulus phase and intensity coding in the cochlear nucleus of the barn owl. J. Neurosci. *4:*1787–1799.

Takahashi, T.T., and M. Konishi (1988a) Projections of the cochlear nuclei and nucleus laminaris to the inferior colliculus of the barn owl. J. Comp. Neurol. *274:*190–211.

Takahashi, T.T., and M. Konishi (1988b) Projections of nucleus angularis and nucleus laminaris to the lateral lemniscal nucleus complex of the barn owl. J. Comp. Neurol. *274:*212–238.

Takahashi, T., A. Moiseff, and M. Konishi (1984) Time and intensity cues are processed independently in the auditory system of the owl. J. Neurosci. *4:*1781–1786.

Thompson, G.C., A.M. Cortez, and D. Man-Kit Lam (1985) Localization of GABA immunoreactivity in the auditory brainstem of guinea pigs. Brain Res. *339:*119–122.

von Bartheld, C.S., R.A. Code, and E.W Rubel (1989) GABAergic neurons in brainstem auditory nuclei of the chick: Distribution, morphology, and connectivity. J. Comp. Neurol. *287:*470–483.

Warchol, M.E., and P. Dallos (1990) Neural coding in the chick cochlear nucleus. J. Comp. Physiol. A *166:*721–734.

Warr, W.B. (1966) Fiber degeneration following lesions in the anterior ventral cochlear nucleus of the cat. Exp. Neurol. *14:*453–474.

Wenthold, R.J., J.M. Zempel, M.H. Parakkal, K.A. Reeks, and R.A. Altschuler (1986) Immunocytochemical localization of GABA in the cochlear nucleus of the guinea pig. Brain Res. *380:*7–18.

Williams, M.N., and R.L.M. Faull (1987) Distribution and morphology of identified thalamocortical projection neurons and glial cells with reference to the question of interneurons in the ventrolateral nucleus of the rat thalamus. Neuroscience *21:*766–780.

Winer, J.A., and D.T. Larue (1988) Anatomy of glutamic acid decarboxylase (GAD) immunoreactive neurons and axons in the rat medial geniculate body. J. Comp. Neurol. *274:*47–68.

Wong-Riley, M.T.T. (1979) Changes in the visual system of monocularly sutured or enucleated cats demonstrable with cytochrome oxidase histochemistry. Brain Res. *171:*11–28.

Young, S.R., and E.W Rubel (1983) Frequency-specific projections of individual neurons in chick brainstem auditory nuclei. J. Neurosci. *3:*1373–1378.

Young, S.R., and E.W Rubel (1986) Embryogenesis of arborization pattern and topography of individual axons in nucleus laminaris of the chicken brain stem. J. Comp. Neurol. *254:*425–459.

Zook, J.M., and R.A. DiCaprio (1988) Intracellular labeling of afferents to the lateral superior olviary nucleus in the bat, *Eptesicus fuscus.* Hearing Res. *34:*141–148.